ELECTRONIC SUPPORTING INFORMATION

Suppression of pyrene excimers through sulfur-bridge oxidation and steric shielding

Vignesh Rajendran[a], K. R. Justin Thomas[a*]

[a]Organic Material Laboratory, Department of Chemistry, Indian Institute of Technology Roorkee, Roorkee, 247667, India.

* Corresponding author: krjt@cy.iitr.ac.in

Table of contents

Instrumentation

The ^{1}H and ^{13}C NMR spectra were recorded in a JEOL 500 MHz spectrometer instrument at 298 K with $CDCl_3$ as a deuterated solvent and TMS as an internal standard. Chemical shifts (δ) are reported in ppm relative to residual solvent signals $CDCl_3$: 7.26 ppm for ^{1}H NMR and 77.10 ppm for ^{13}C NMR. HRMS spectra were acquired on Agilent Mass Hunter Qualitative Analysis 10 Software. UV-Vis absorption spectra for all the final dyes were recorded on a Cary 100 UV-vis spectrophotometer. Fluorescence emission spectra have been recorded in the Horiba Scientific Fluoromax 4C spectrophotometer. The dyes' absolute photoluminescence quantum yield (PLQY) was determined by the calibrated integrating sphere method in the Edinburgh spectrofluorometer. The fluorescence lifetime measurements of liquid, solid, and thin film samples, including fitting, were acquired by the FLS 1000 Edinburgh instrument. FE-SEM Carl Zeiss Ultra Plus was acquired to study the morphology of aggregated samples. All data were collected from a single crystal at 103 K on a Bruker D8 QUEST FIXED CHI diffractometer with a microfocus sealed tube using a multilayer mirror as monochromator and a Bruker PHOTON III CPAD detector. The diffractometer was equipped with an Oxford Cryostream 1000 low temperature device and used Mo K_α radiation (λ = 0.71073 Å). All data were integrated with SAINT V8.42, yielding 36530 reflections of which 4943 where independent (average redundancy 7.39) and 74.0% were greater than $2\sigma(F^2)$. A Multi-Scan absorption correction using SADABS 2016/2 was applied. The structure was solved by Intrinsic Phasing methods with SHELXT 2018/2 and refined by full-matrix least-squares methods against F^2 using SHELXL-2019/2. All non-hydrogen atoms were refined with anisotropic displacement parameters. All hydrogen atoms were refined isotropic on calculated positions using a riding model with their U_{iso} values constrained to 1.5 times the U_{eq} of their pivot atoms for terminal sp^3 carbon atoms and 1.2 times for all other carbon atoms. An electrochemical analyzer with a three-electrode set up (glassy carbon as working electrode,

non- aqueous $Ag/AgNO_3$ as reference electrode, and platinum auxiliary electrode) was used to record cyclic voltammetry (CV) and differential pulse voltammetry (DPV) with ferrocene as internal standard and tetrabutylammonium perchlorate as supporting electrolyte using BASi Epsilon electrochemical analyzer. The thermal stability of dyes was observed by thermogravimetric analysis (TGA) using a Perkin–Elmer Pyris diamond analyzer instrument with a heating rate of 10°C/min and by maintaining a nitrogen atmosphere.

Materials

All the required chemicals were purchased from the available commercial sources and used without further purification. Pyrene, *p*-toluene thiol, *m*CPBA, Cs_2CO_3, all other reagents and solvents were purchased and utilized without further purification from Sigma Aldrich, TCI, and SRL chemicals. All the solvents were distilled using the appropriate distillation set up for further studies. Precoated alumina plates from Merck grade were used for thin layer chromatography (TLC) analysis. All the compounds were purified using column chromatography over silica gel having mesh sizes ranging from 200-400. Caution! Precautions should be taken while handling Liq. Br_2 and *p*-toluenethiol as described in their SDSs.

Experimental section

Density Functional Theoretical Calculations

All the theoretical calculations were performed using ORCA 6.0.1 software[1] at the B3LYP/def2-svp level. The geometries of the lowest excited singlet (S_1) and triplet (T_1) states were optimized by TD-DFT. The global minima of the optimized structures were confirmed by frequency calculation on the optimized structures which showed no negative frequencies. TD-DFT calculations at the B3LYP/def2-tzvp level on the optimized structures were performed to estimate the excitation energies, singlet-triplet energy gap and other relevant parameters. Natural transition orbitals (NTO) and the charge transfer indices were calculated using a Multiwfn program.[2]

Crystallization procedure

All the crystal was obtained by solvent vapor diffusion technique. For this, each final dye around 5 mg were dissolved in dry DCM and over poor solvent hexane was layered carefully at room temperature for further crystallization process.

Preparation for thin film

All the final dyes around 2 mg were dissolved in toluene. Further drop cast on quartz plate followed slow evaporation at room temperature.

Synthesis procedures

Synthesis of precursors: 1

1 was synthesized by following reported protocol.[3] In a 250 mL RB flask, compound pyrene (25 g, 123 mmol) was dissolved in dry MC (100 mL) and cooled at 0 ^{o}C. Afterward, $AlCl_3$ (16.5 g, 123 mmol, 1 equiv.) was added in one portion at the same temperature. Finally, dropwise *t*-BuCl (13.4 mL, 123 mmol, 1 eq) was added to the mixture under N_2 atm. Then, the brown mixture was shifted to room temperature and allowed to stir for 3 hours. After completing reaction hours, excess of $AlCl_3$ was quenched by adding sat. $NaHCO_3$ solution. Then, the organic phase was extracted with MC, dried over anhydrous sodium sulfate, and concentrated by rotary evaporation. Finally, the crude product was purified by column chromatography (eluant: 100% Hexane) and obtained as colourless solid having a 77% yield.

Synthesis of precursors: 2

2 was synthesized by following reported protocol.[4] In a flask, **1** (5 g, 19.35 mmol) in DCM (100 mL) was maintained at -78 ^{o}C. Afterward, Br_2 (0.9 mL, 17.417 mmol, 1 equiv.) in DCM (40 mL) was added dropwise to the mixture at the same temperature over 30 minutes and then stirred for 15 hours at room temperature. After completing reaction hours, the mixture was quenched by sat. $Na_2S_2O_5$ solution (10 mL). The precipitate was collected under a vacuum and

washed with methanol (40 mL). Finally, the crude product was washed with hexane (20 mL), which yielded the white solid (4.8 g, 60% yield), and proceeded without any further purification. ^{1}H NMR (500 MHz, $CDCl_3$) δ 8.39 (d, *J* = 9.2 Hz, 1H), 8.26 – 8.23 (m, 2H), 8.19 – 8.13 (m, 2H), 8.06 (d, *J* = 8.9 Hz, 1H), 7.98 (t, *J* = 8.8 Hz, 2H), 1.58 (d, *J* = 0.8 Hz, 9H).

Synthesis of PS

In 100 mL double neck RB flask, a **2** (1.87 g, 5.54 mmol) and *p*-toluene thiol (1 g, 8.35 mmol, 1.5 equiv.) and Cs_2CO_3 (2.73 g, 8.35 mmol, 1.5 equiv.) was dissolved in 20 mL of DMF. Further, the mixture was purged with N_2 over 5 minutes of stirring. Afterward, the mixture was heated at 110 °C for 15 hours at N_2 atm. After the completion, the reaction mixture was brought to room temperature and poured into crushed ice. Then, the precipitate was collected and dried under a vacuum. Finally, the crude product was purified by column chromatography (eluant: 5% DCM/Hexane) and obtained as a white crystalline solid with 64% yield. Melting point 134.7 °C. IR (KBr) cm^{-1}: 3019, 2956, 2923, 2854, 1589, 796. ^{1}H NMR (500 MHz, $CDCl_3$) δ 8.63 (d, *J* = 9.2 Hz, 1H), 8.25 (s, 2H), 8.12 (d, *J* = 9.3 Hz, 1H), 8.10 – 8.05 (m, 3H), 8.04 – 8.01 (m, 1H), 7.17 – 7.12 (m, 2H), 7.08 – 7.02 (m, 2H), 2.30 (s, 3H). ^{13}C NMR (125 MHz, $CDCl_3$) δ 149.45, 136.20, 133.69, 131.62, 131.13 (d, *J* = 10.6 Hz), 130.83, 129.90, 129.48, 128.90, 128.54, 128.09, 127.08, 124.94, 124.64, 122.72 (d, *J* = 12.2 Hz), 35.22, 31.88, 20.98. HRMS Calculated mass $C_{27}H_{24}S$ (M+): 380.1613, Exact mass $C_{27}H_{24}OS$ (M+): 380.1606.

Synthesis of PSO

In a 100 mL RB flask, a compound **PS** (200 mg, 0.52 mmol) was dissolved in 10 mL of DCM at 0 °C. Afterward, *m*CPBA (108 mg, 0.60 mmol, 1.2 equiv.) was added slowly to the mixture at the same temperature. Further, the resultant mixture was stirred at 0 °C for 30 minutes. Afterward, the mixture was quenched with sat. K_2CO_3 solution. Then, the organic layer was extracted by DCM and dried over anhydrous sodium sulfate. Finally, the crude product was purified by column chromatography (eluant: 80% DCM/Hexane) and obtained as a light green solid with a yield of (200 mg) 96%. Melting point 205.1 °C. IR (KBr) cm^{-1}: 3013, 2963, 2921,

2854, 1590, 1081, 1055, 804. ^{1}H NMR (500 MHz, $CDCl_3$) δ 8.55 (dd, *J* = 15.0, 8.6 Hz, 2H), 8.30 – 8.25 (m, 3H), 8.15 (dd, *J* = 14.1, 9.1 Hz, 2H), 8.05 (d, *J* = 8.9 Hz, 1H), 7.57 (d, *J* = 8.3 Hz, 2H), 7.16 (dt, *J* = 8.0, 0.7 Hz, 2H), 2.28 (s, 3H), 1.58 (s, 9H). ^{13}C NMR (125 MHz, $CDCl_3$) δ 149.90, 142.66, 141.18, 137.29, 133.05, 130.97, 130.24, 129.90, 129.41 (d, *J* = 5.5 Hz), 127.07, 125.15 (d, *J* = 33.8 Hz), 123.63 (d, *J* = 19.9 Hz), 121.82, 121.22, 35.28, 31.84, 21.27. HRMS Calculated mass $C_{27}H_{24}OS$ $(M+H)^+$: 397.1626, Exact mass $C_{27}H_{24}OS$ $(M+H)^+$: 397.1632.

Synthesis of PSO_2

In a 100 mL RB flask, a compound **PS** (500 mg, 1.31 mmol) was dissolved in 20 mL of DCM at 0 °C. Afterward, *m*CPBA (1.1 g, 6.50 mmol, 5 equiv.) was added slowly to the mixture at the same temperature. Further, the resultant mixture was stirred at 0 °C for 1 hour. Afterward, the mixture was quenched with sat. K_2CO_3 solution. Then, the organic layer was extracted by DCM and dried over anhydrous sodium sulfate. Finally, the crude product was purified by column chromatography (eluant: 95% DCM/Hexane) and obtained as a light green solid with a yield of (410 mg) 75%. Melting point 327.3 °C. IR (KBr) cm^{-1}: 3036, 2956, 2922, 2859, 1585, 1155, 1126, 665. ^{1}H NMR (500 MHz, $CDCl_3$) δ 8.96 (d, *J* = 9.4 Hz, 1H), 8.88 (d, *J* = 8.2 Hz, 1H), 8.33 – 8.28 (m, 2H), 8.25 (d, *J* = 8.3 Hz, 1H), 8.19 (dd, *J* = 9.2, 4.7 Hz, 2H), 8.07 (d, *J* = 8.9 Hz, 1H), 7.92 – 7.85 (m, 2H), 7.22 (dd, *J* = 8.5, 0.7 Hz, 2H), 2.31 (s, 3H), 1.57 (s, 9H). ^{13}C NMR (125 MHz, $CDCl_3$) δ 151.22, 144.32, 138.76, 133.18, 131.99, 129.88, 127.62, 126.38, 122.59, 35.34, 31.68, 21.52. HRMS Calculated mass $C_{27}H_{24}O_2S$ (M+): 412.1497, Exact mass $C_{27}H_{24}O_2S$ (M+): 412.1488.

Photophysical studies

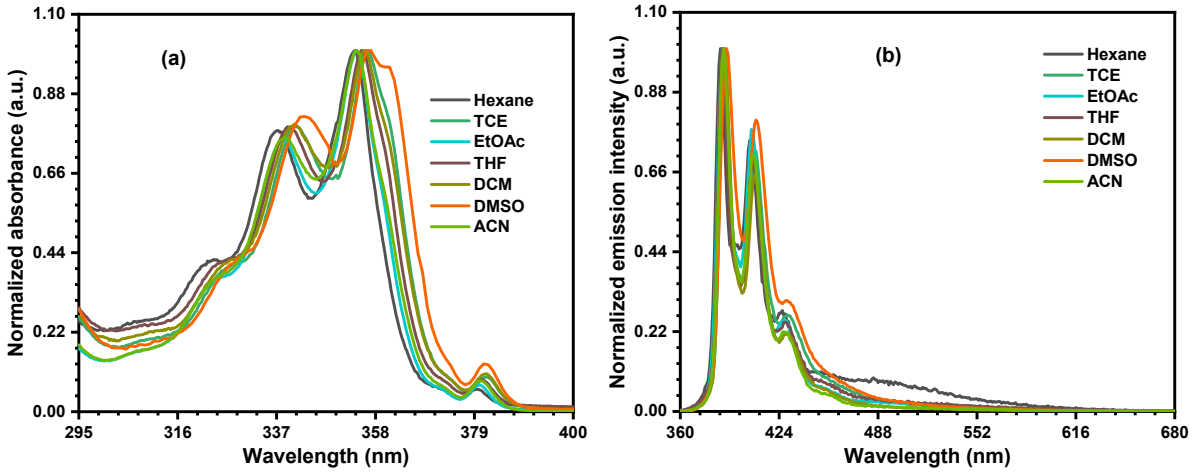

Fig. S1. (a) Absorption, (b) emission spectra of **PSO** recorded in different solvents.

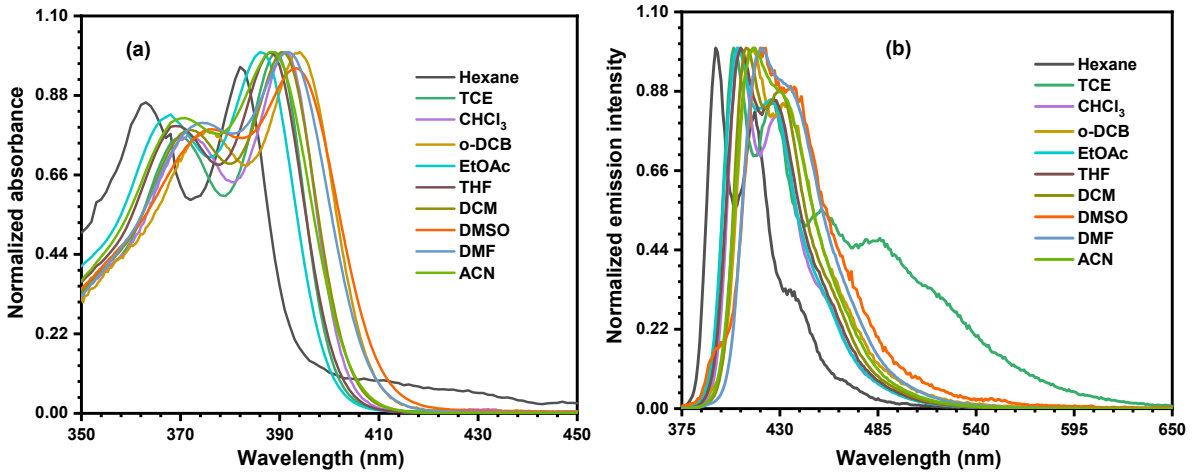

Fig. S2. (a) Absorption, (b) emission spectra of **PSO_2** recorded in different solvents.

Table S1. Solvatochromic data of **PS** in various solvents.

Solvent	E^N_T	Orientation Polarizability (Δf)	λ_{abs} (nm)	λ_{em} (nm)	Stokes Shift (nm)	Δν (cm^{-1})
Hex	0.009	0.012	353	385	32	2354.58
Tol	0.099	0.014	356	388	32	2316.69
TEA	0.043	0.045	354	388	34	2475.39
TCE	0.160	0.085	356	389	33	2382.94
***o*DCB**	0.225	0.186	357	391	34	2435.75
EtOAc	0.228	0.199	353	387	34	2488.81
THF	0.207	0.210	355	388	33	2395.81
DMSO	0.444	0.263	356	391	35	2514.44
DMF	0.386	0.276	355	389	34	2462.07
ACN	0.460	0.305	354	389	35	2541.64

Table S2. Solvatochromic data of **PSO** in various solvents.

Solvent	E^N_T	Orientation Polarizability (Δf)	λ_{abs} (nm)	λ_{em} (nm)	Stokes Shift (nm)	Δν (cm^{-1})
Hex	0.009	0.012	350	396	46	3318.90
TCE	0.160	0.085	354	401	47	3310.93
EtOAc	0.228	0.199	352	399	47	3346.43
THF	0.207	0.210	353	400	47	3328.61
DCM	0.309	0.217	353	420	67	4519.08
DMSO	0.444	0.263	356	422	66	4393.20
ACN	0.460	0.305	366	594	228	10487.3

Table S3. Solvatochromic data of **PSO_2** in various solvents.

Solvent	E^N_T	Orientation Polarizability (Δf)	λ_{abs} (nm)	λ_{em} (nm)	Stokes Shift (nm)	Δν (cm^{-1})
Hex	0.009	0.012	383	394	11	728.94
TCE	0.160	0.085	389	404	15	954.46
$CHCl_3$	0.259	0.149	391	407	16	1005.42
***o*DCB**	0.225	0.186	393	413	20	1232.21
EtOAc	0.228	0.199	386	406	20	1276.19
THF	0.207	0.210	389	408	19	1197.13
DCM	0.309	0.217	390	411	21	1310.12
DMSO	0.444	0.263	393	420	27	1635.76
DMF	0.386	0.276	391	420	29	1765.92
ACN	0.460	0.305	388	415	27	1676.81

Table S4. Solvatochromic properties of all dyes.

Dye	Chemical formula	R^2	Onsager radius	Slope	Δμ
PS	$C_{27}H_{24}S$	0.88	4.36 A°	1579.559	3.61 D
PS	$C_{27}H_{24}S$	0.96	4.36 A°	12404.338	10.13 D
PSO	$C_{27}H_{24}SO$	0.93	4.40 A°	633.4935	2.31 D
PSO_2	$C_{27}H_{24}O_2S$	0.89	4.46 A°	3471.5291	5.53 D

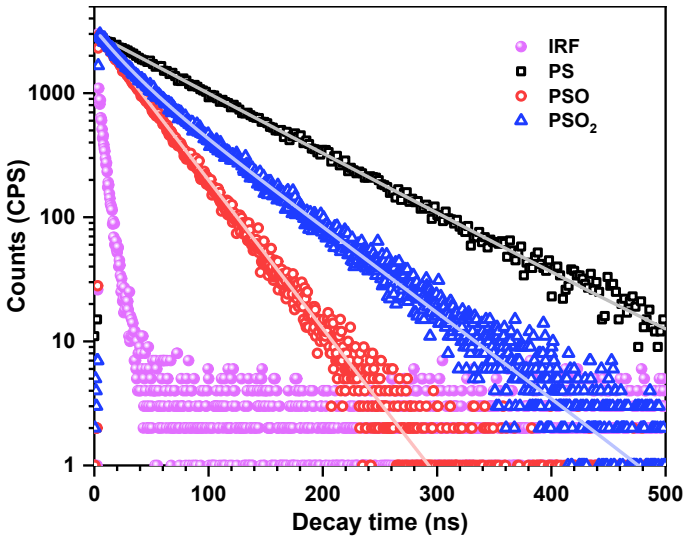

Figure S3. Lifetime decay of all dyes in solids.

Table S5. Lifetime decay of all dyes in solution, thin film and solid.

	Dyes	τ_1 (ns)	τ_2 (ns)	Average τ (ns)	χ^2
Solution	PS	1.75	-	1.75	1.0
	PSO	1.34	-	1.34	0.95
	PSO_2	3.30	-	3.30	0.99
Thin film	PS	13.99	26.51	21.35	1.08
	PSO	8.61	25.57	22.25	1.12
	PSO_2	25.0	70.29	68.16	1.10
Solid	PS	89.86	-	89.86	1.03
	PSO	36.3	-	36.3	0.90
	PSO_2	24.04	63.02	55.93	1.10

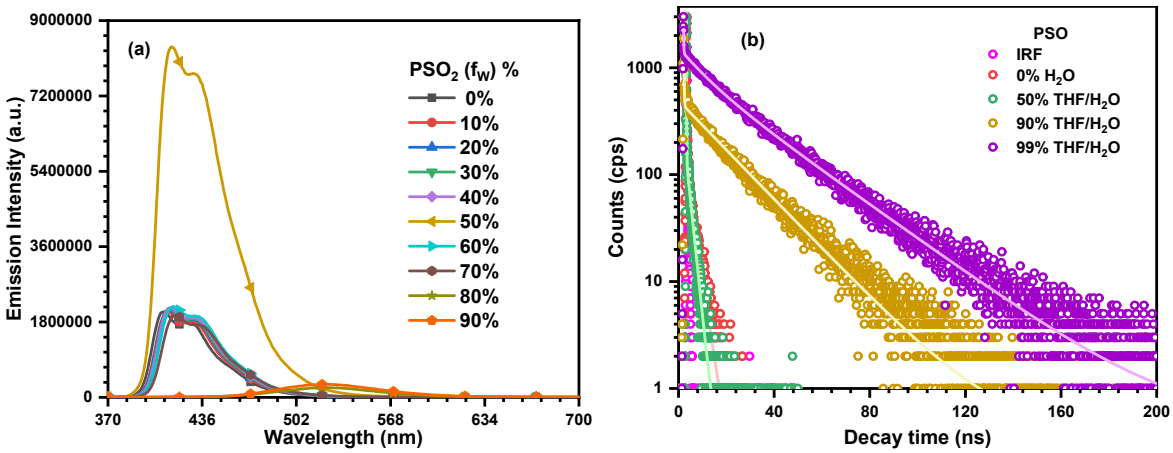

Figure S4. (a) AIE study of **PSO_2**, (b) Lifetime decay of aggregated **PSO** dye.

Table S6. Lifetime decay of all dyes in various water fractions

Compound	Fraction	τ (ns)	χ^2
PS	0% H_2O	1.7548	1.0153
	50% THF/H_2O	2.1308	1.0263
	90% THF/H_2O	12.0375	1.0132
	99% THF/H_2O	22.7001	1.0795
PSO	0% H_2O	1.3416	1.0767
	50% THF/H_2O	0.9523	0.9649
	90% THF/H_2O	17.9838	1.0525
	99% THF/H_2O	24.3942	1.0977
PSO_2	0% H_2O	3.3004	1.0222
	50% THF/H_2O	3.2814	1.0101
	90% THF/H_2O	72.8975	0.9742
	99% THF/H_2O	65.0691	0.9459

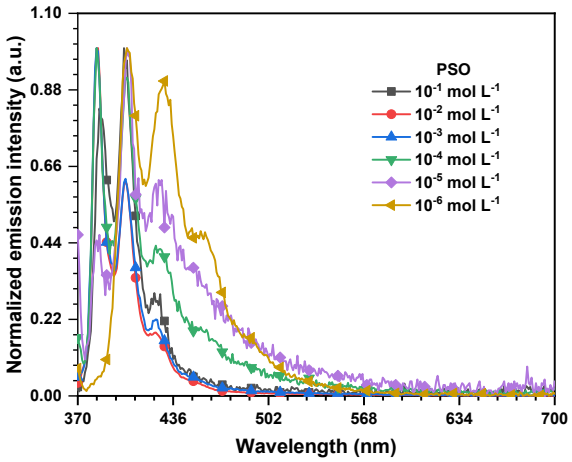

Figure S5. Concentration dependent emission of **PSO**.

Table S7. Kinetic parameter of all dyes in various water fractions

Compound	Fraction	PLQYs (%)	τ (ns)	K_r (s)	k_{nr} (s)
PS	0% H_2O	18.09	1.75	1.03 x 10^8 s^{-1}	4.68 x 10^8 s^{-1}
	99% THF/H_2O	85.19	22.70	3.75 x 10^7 s^{-1}	6.52 x 10^7 s^{-1}
PSO	0% H_2O	14.25	1.34	1.06 x 10^8 s^{-1}	6.40 x 10^8 s^{-1}
	99% THF/H_2O	78.58	24.39	3.23 x 10^7 s^{-1}	8.82 x 10^6 s^{-1}

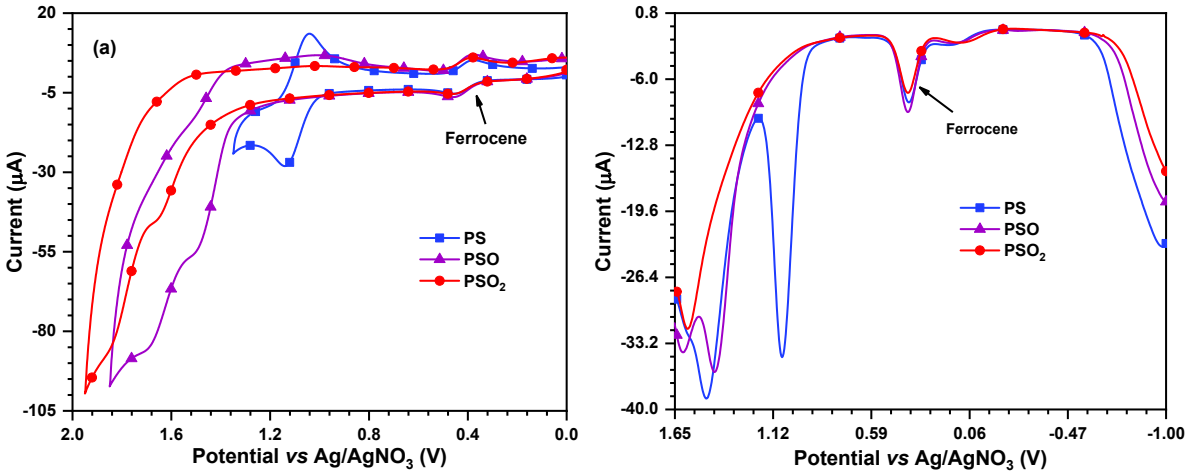

Figure S6. (a) Cyclic voltammetry and **(b)** DPV of all dyes recorded in DCM.

Theoretical studies

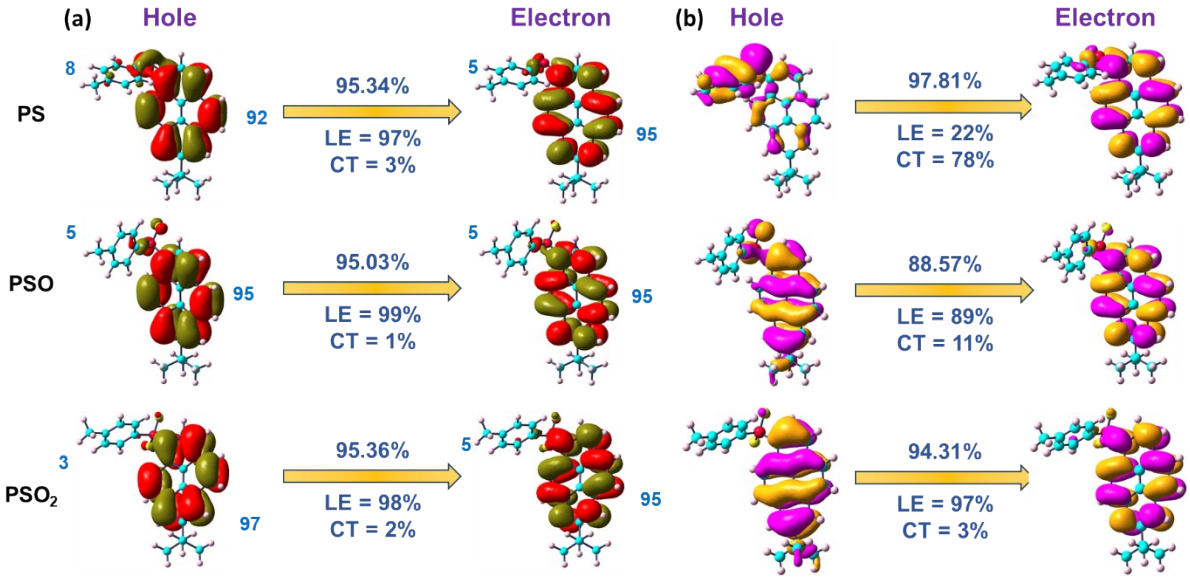

Figure S7. NTO analysis of all dyes depicted in state **(a)** T_1 and **(b)** T_2 state.

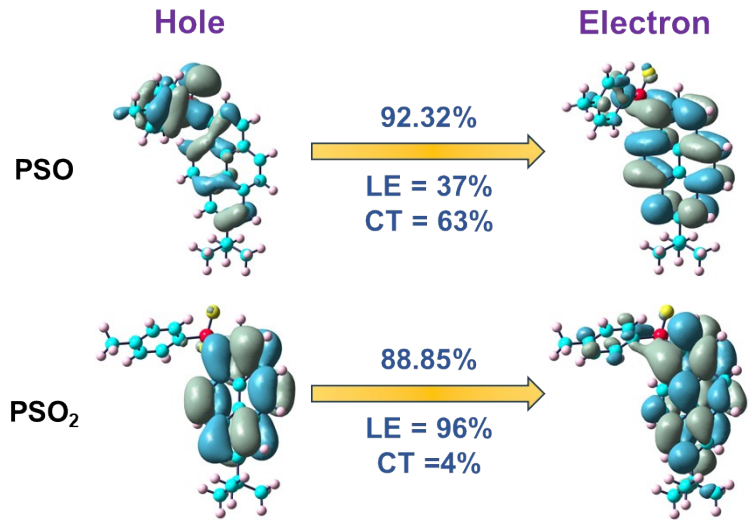

Figure S8. NTO analysis of all dyes depicted in state T_3 state.

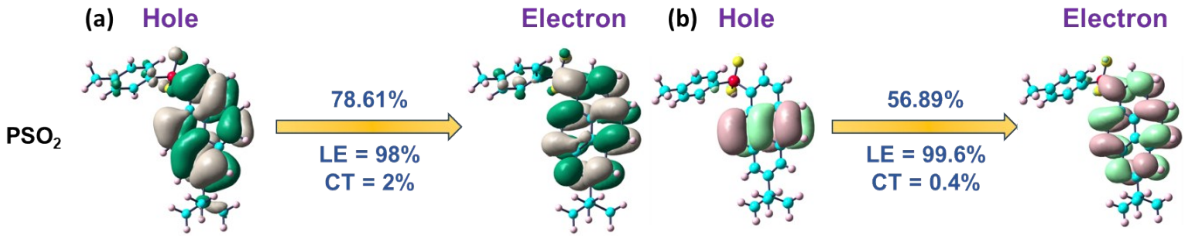

Figure S9. NTO analysis of all dyes depicted in state S_2 and T_4 state.

Table S8. HOMO–LUMO fragment contributions and hole–electron distribution parameters for S_1 and T_1 states of **PS, PSO**, and **PSO_2**.

Compound	Fragment	HOMO	LUMO	S_1				T_1			
				HOLE	ELECTRON	%CT	%LE	HOLE	ELECTRON	%CT	%LE
PS	C1-C37	58.114	41.885	13.48	93.66	80.18	19.81	91.54	94.90	3.35	96.64
	C38-C52	94.858	5.137	86.52	6.34			8.46	5.10		
PSO	C1-C37	88.755	11.228	27.93	94.10	66.17	33.82	94.58	95.34	0.75	99.24
	C38-C53	94.804	5.175	72.07	5.90			5.42	4.66		
PSO_2	C1-C37	96.191	3.801	96.91	88.66	8.26	91.73	96.56	94.66	1.89	98.10
	C38-C54	92.775	7.216	3.23	11.49			3.44	5.34		

Table S9. HOMO–LUMO fragment contributions and hole–electron distribution parameters for T_2 and T_3 states of **PS, PSO**, and **PSO_2**.

Compound	Fragment	T_2				T_3			
		HOLE	ELECTRON	%CT	%LE	HOLE	ELECTRON	%CT	%LE
PS	C1-C37	15.50	94.00	78.49	21.50	95.61	97.27	1.65	98.34
	C38-C52	84.50	6.00			4.39	2.73		
PSO	C1-C37	85.96	96.62	10.66	89.33	28.58	92.01	63.42	36.57
	C38-C53	14.04	3.38			71.42	7.99		
PSO_2	C1-C37	99.18	96.17	3.00	96.99	97.39	93.83	3.56	96.43
	C38-C54	0.82	3.83			2.61	6.17		

Table S10. HOMO–LUMO fragment contributions and hole–electron distribution parameters for T_4 and T_5 states of **PS, PSO**, and **PSO_2**.

Compound	Fragment	T_4				T_5			
		HOLE	ELECTRON	%CT	%LE	HOLE	ELECTRON	%CT	%LE
PSO	C1-C37	94.75	97.52	2.77	97.22	98.63	98.58	0.04	99.95
	C38-C53	5.25	2.48			1.37	1.42		
PSO_2	C1-C37	97.95	97.89	0.06	99.94	48.62	49.01	0.38	99.61
	C38-C54	2.05	2.11			51.38	50.99		

Table S11. HOMO–LUMO fragment contributions and hole–electron distribution parameters for S_2 states of **PS, PSO**, and **PSO_2**.

Compound	Fragment	S_2			
		HOLE	ELECTRON	%CT	%LE
PSO_2	C1-C37	95.03	93.25	1.77	98.22
	C38-C54	4.97	6.75		

Crystallographic data

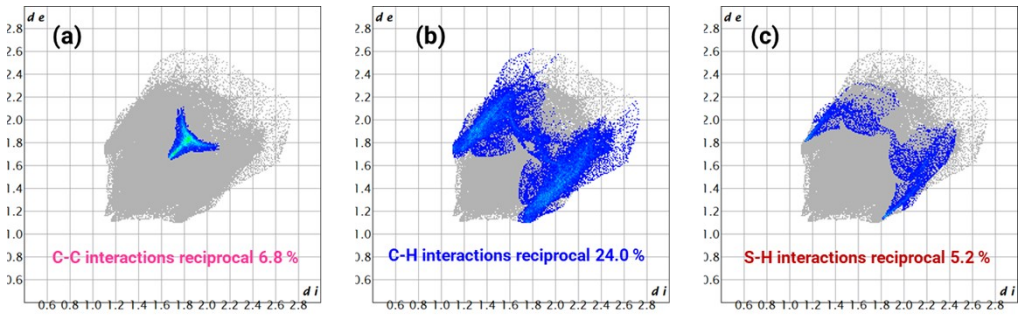

Figure S10. Decomposed Hirshfeld surface plots of **PS** showing contributions from **(a) C···C**, **(b) C···H**, and **(c) S···H** interactions.

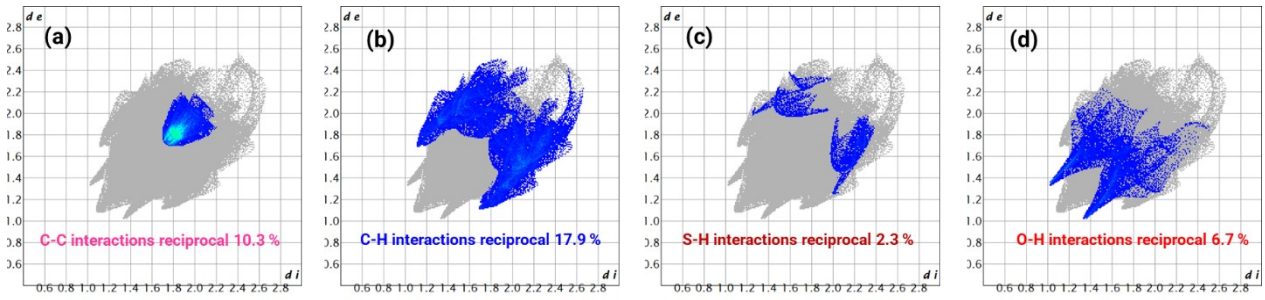

Figure S11. Decomposed Hirshfeld surface plots of **PSO** showing contributions from **(a) C···C**, **(b) C···H**, **(c) S···H,** and **(d) O···H** interactions.

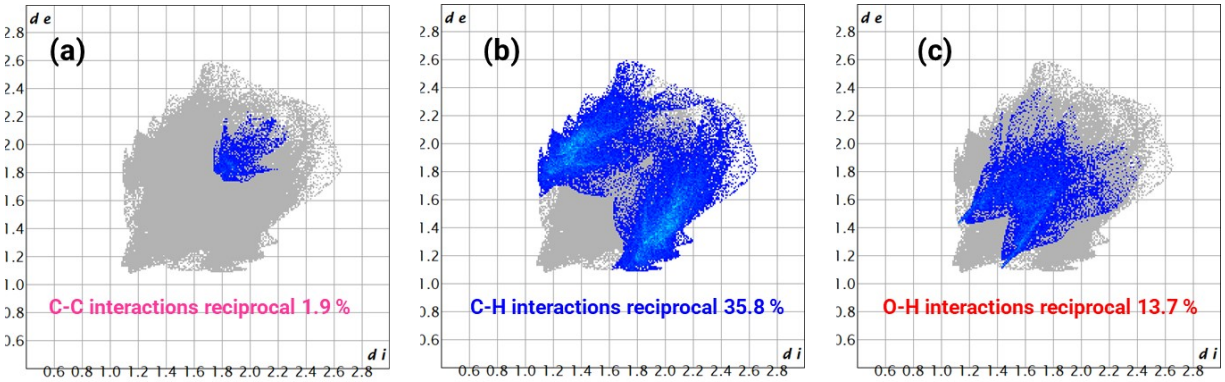

Figure S12. Decomposed Hirshfeld surface plots of **PSO_2** showing contributions from **(a) C···C**, **(b) C···H**, and **(c) O···H** interactions.

Table S12. Crystal data and structure refinement for **PS**

CCDC No	2530247
Empirical formula	$C_{27}H_{24}S$
Formula weight	380.52
Temperature/K	100.00
Crystal system	monoclinic
Space group	$P2_1/c$
a/Å	11.874(2)
b/Å	10.5176(18)
c/Å	16.424(3)
α/°	90
β/°	98.126(5)
γ/°	90
Volume/Å^3	2030.5(6)
Z	4
ρ_{calc}g/cm^3	1.245
μ/mm^{-1}	0.169
F(000)	808.0
Crystal size/mm^3	0.238 × 0.083 × 0.035
Radiation	MoKα (λ = 0.71073)
2Θ range for data collection/°	3.464 to 52.988
Index ranges	-14 ≤ h ≤ 14, -13 ≤ k ≤ 13, -20 ≤ l ≤ 20
Reflections collected	42661
Independent reflections	4211 [R_{int} = 0.0654, R_{sigma} = 0.0343]
Data/restraints/parameters	4211/0/257
Goodness-of-fit on F^2	1.061
Final R indexes [I>=2σ (I)]	R_1 = 0.0412, wR_2 = 0.1048
Final R indexes [all data]	R_1 = 0.0482, wR_2 = 0.1115
Largest diff. peak/hole / e Å^{-3}	0.32/-0.22

Table S13. Crystal data and structure refinement for **PSO**

CCDC number	2530815
Empirical formula	$C_{27}H_{24}OS$
Formula weight	396.52
Temperature [K]	103(2)
Crystal system	monoclinic
Space group (number)	$P2_1/n$ (14)
a [Å]	7.4237(3)
b [Å]	29.7475(12)
c [Å]	9.1816(4)
α [°]	90
β [°]	90.311(2)
γ [°]	90
Volume [Å^3]	2027.60(15)
Z	4
ρ_{calc} [gcm^{-3}]	1.299
μ [mm^{-1}]	0.176
F(000)	840
Crystal size [mm^3]	0.093×0.134×0.203
Crystal colour	colourless
Crystal shape	block
Radiation	Mo K_α (λ=0.71073 Å)
2θ range [°]	5.21 to 56.26 (0.75 Å)
Index ranges	$-9 \le h \le 9$ $-39 \le k \le 33$ $-10 \le l \le 12$
Reflections collected	36530
Independent reflections	4943 R_{int} = 0.0678 R_{sigma} = 0.0523
Completeness to θ = 25.242°	99.8
Data / Restraints / Parameters	4943 / 0 / 266
Goodness-of-fit on F^2	1.033
Final R indexes [$I \ge 2\sigma(I)$]	R_1 = 0.0596 wR_2 = 0.1497
Final R indexes [all data]	R_1 = 0.0828 wR_2 = 0.1656
Largest peak/hole [eÅ^{-3}]	1.12/−0.40

Table S14. Crystal data and structure refinement for **PSO_2**

CCDC No	2530246
Empirical formula	$C_{27}H_{24}O_2S$
Formula weight	412.52

Temperature/K	100.00
Crystal system	orthorhombic
Space group	Pbca
a/Å	18.3088(9)
b/Å	6.8770(3)
c/Å	32.6593(16)
α/°	90
β/°	90
γ/°	90
Volume/Å^3	4112.1(3)
Z	8
ρ_{calc}g/cm^3	1.333
μ/mm^{-1}	0.179
F(000)	1744.0
Crystal size/mm^3	0.424 × 0.038 × 0.037
Radiation	MoKα (λ = 0.71073)
2Θ range for data collection/°	2.494 to 52.74
Index ranges	-22 ≤ h ≤ 22, -8 ≤ k ≤ 8, -40 ≤ l ≤ 40
Reflections collected	49108
Independent reflections	4219 [R_{int} = 0.0595, R_{sigma} = 0.0303]
Data/restraints/parameters	4219/0/275
Goodness-of-fit on F^2	1.086
Final R indexes [I>=2σ (I)]	R_1 = 0.0414, wR_2 = 0.1063
Final R indexes [all data]	R_1 = 0.0499, wR_2 = 0.1135
Largest diff. peak/hole / e Å^{-3}	0.42/-0.30

Table S15. Selected bond lengths and angles observed in **PS**, **PSO** and **PSO_2**

Compound	C-S, Å	S=O, Å	C-S-C, °	C-S-C-C, °
PS	1.7715(12)	-	103.47(6), 106.33(6)	-100.57(10), 84.24(11)
PSO	1.794(2)	1.4806(18)	98.55(10)	146.12(18), −39.5(2)
PSO_2	1.7747(16)	1.4415(12)	105.62(8)	-113.49(14), 69.27(14)

NMR Spectrum

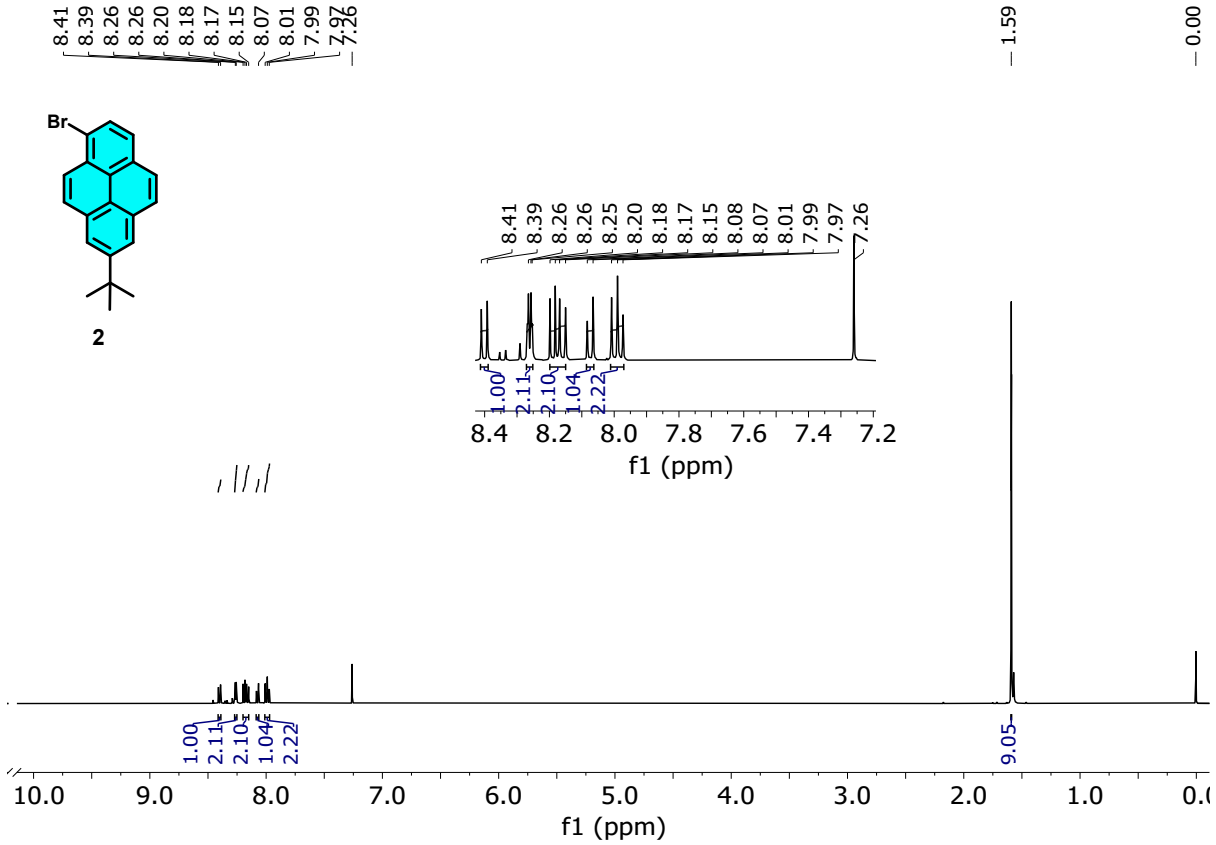

Figure S13. ^{1}H NMR (500 MHz, $CDCl_3$) of **2.**

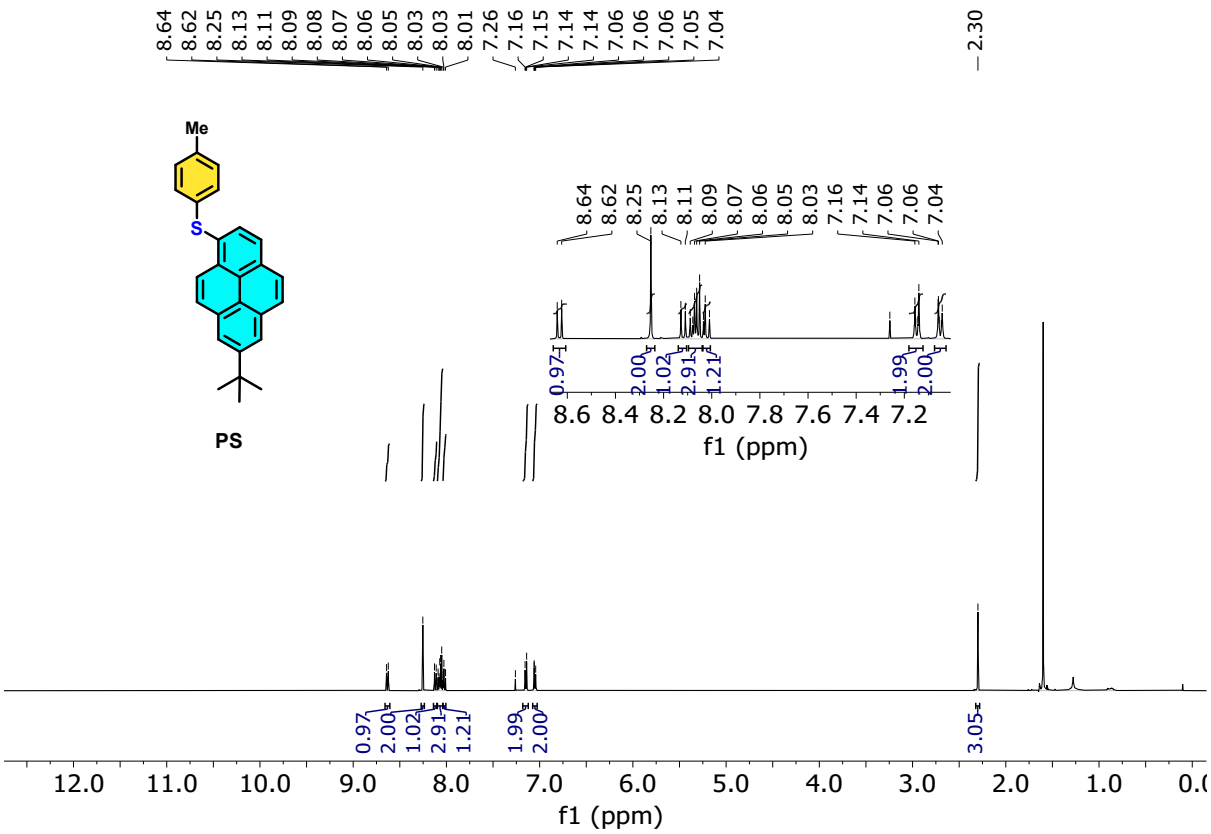

Figure S14. ^{1}H NMR (500 MHz, $CDCl_3$) of **PS.**

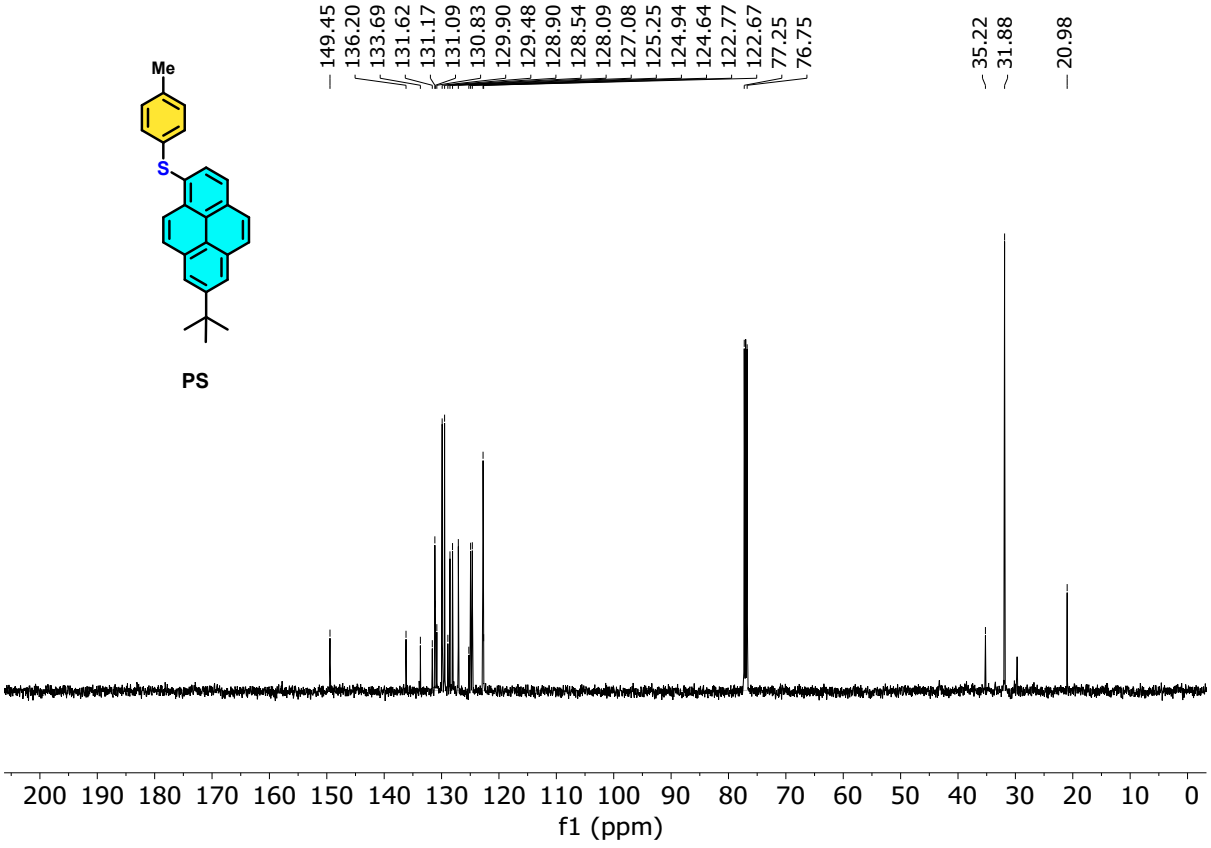

Figure S15. ^{13}C NMR (125 MHz, $CDCl_3$) of **PS.**

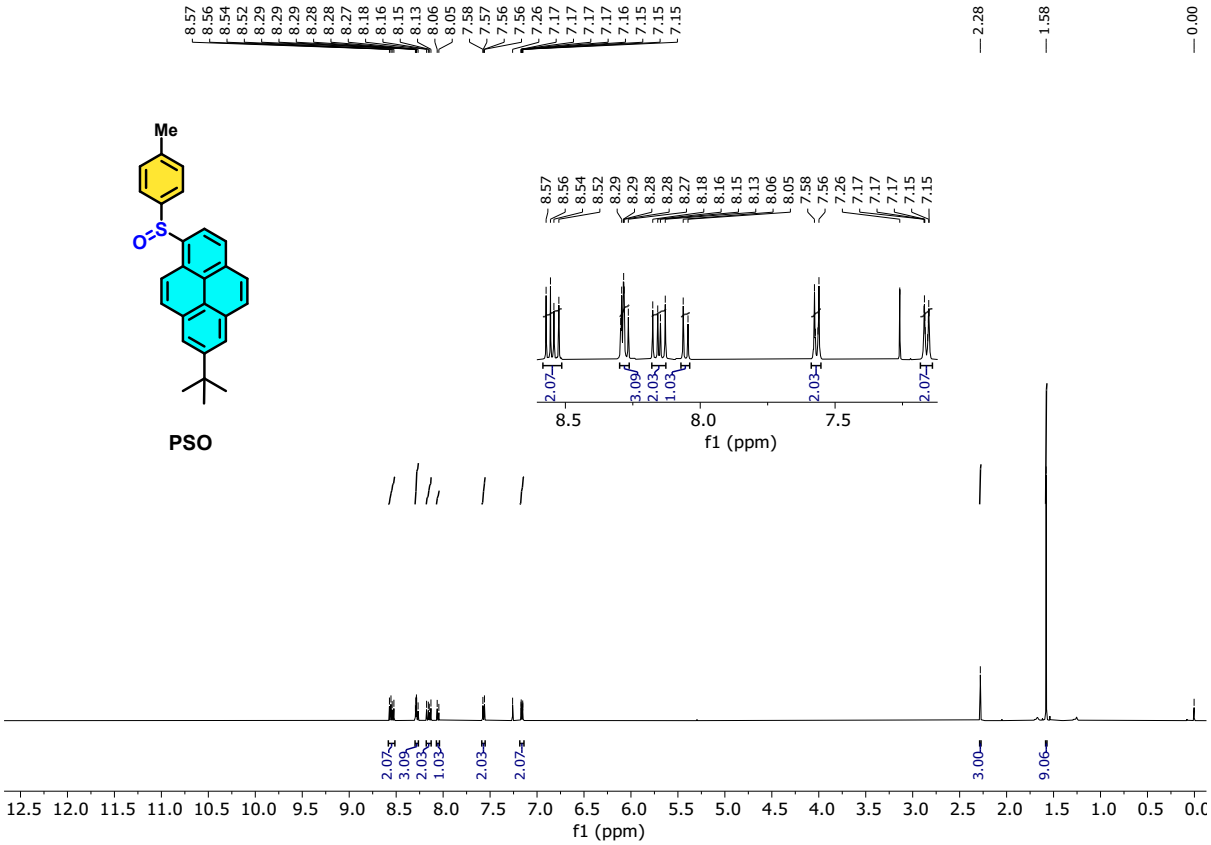

Figure S16. ^{1}H NMR (500 MHz, $CDCl_3$) of **PSO.**

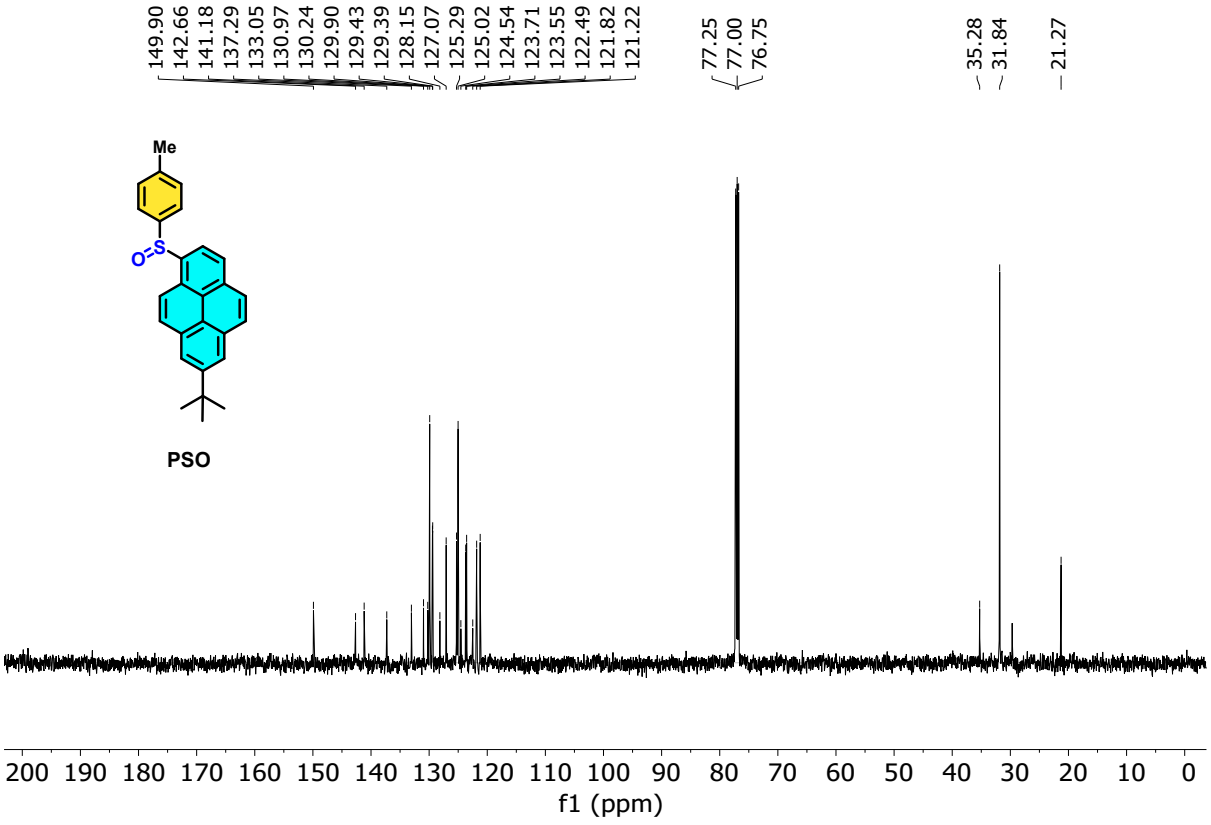

Figure S17. ^{13}C NMR (125 MHz, $CDCl_3$) of **PSO.**

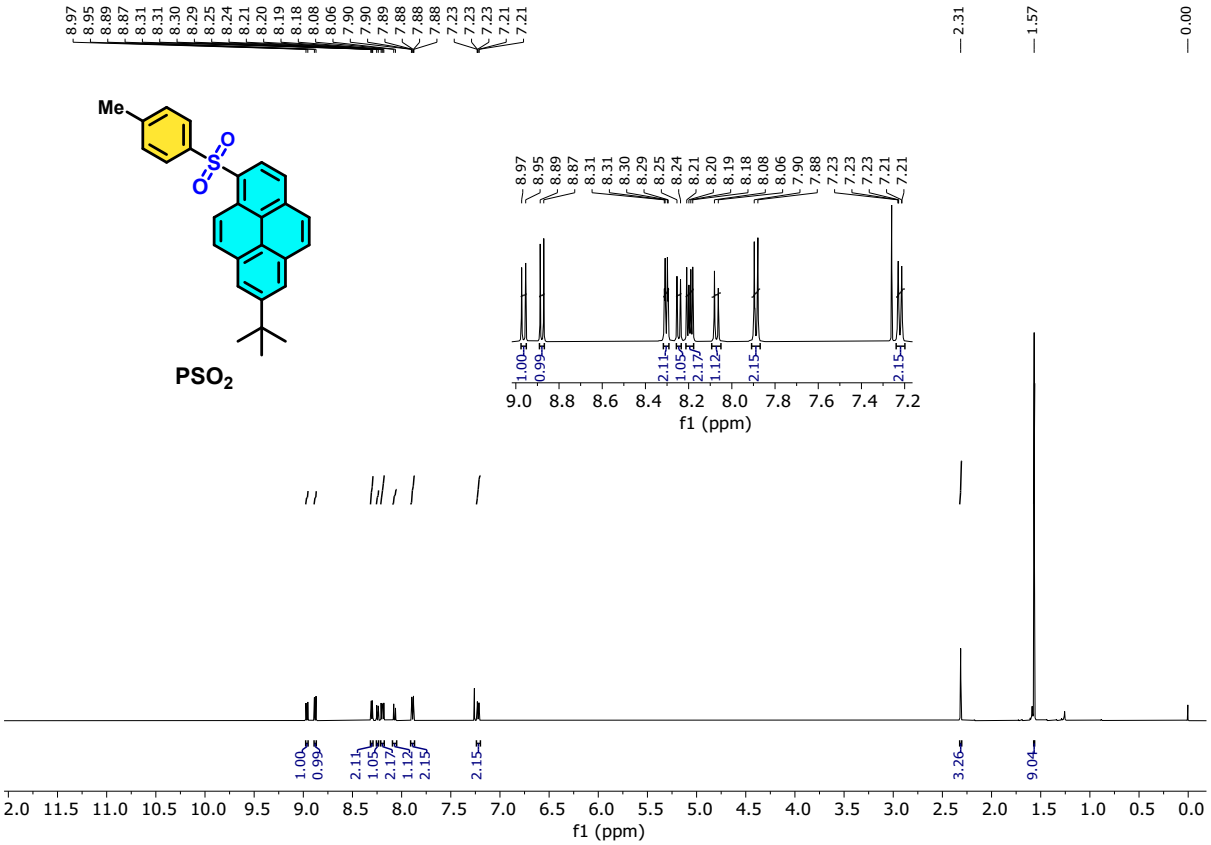

Figure S18. ^{1}H NMR (500 MHz, $CDCl_3$) of **PSO_2.**

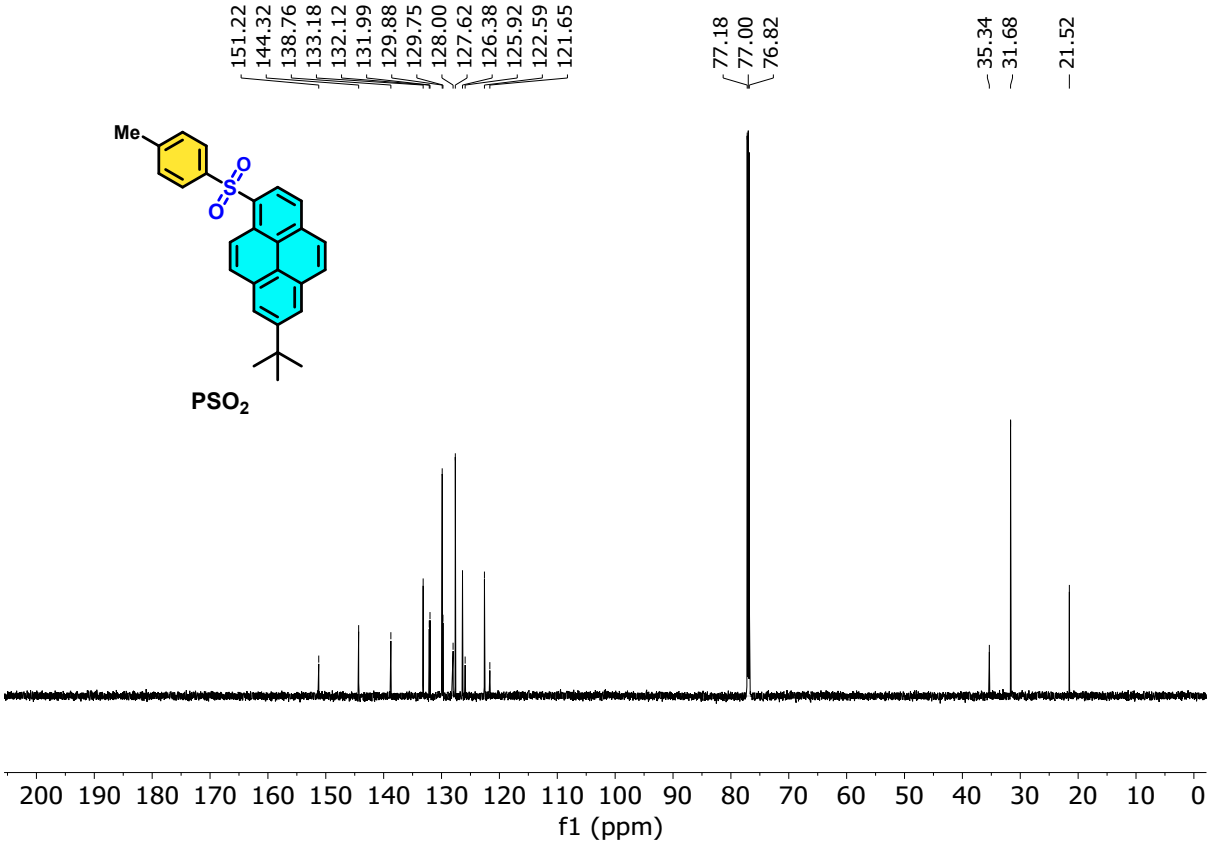

Figure S19. ^{13}C NMR (125 MHz, $CDCl_3$) of **PSO_2.**

References

1. F. Neese, *Wiley Interdiscip. Rev.: Comput. Mol. Sci*., 2025, **15**, 2, e70019.
2. T. Lu, *J. Chem. Phys.*, 2024, **161**, 082503.
3. L. Djordjevic, C. Valentini, N. Demitri, C. Meziere, M. Allain, M. Salle, A. Folli, D. Murphy, S. Manas-Valero, E. Coronado, D. Bonifazi, *Angew. Chem., Int. Ed.*, 2020, ***59***, 4106-4114.
4. J. Han, L. Wang, Y. Zhang, Y. Li, J. Wang, *Org. Lett.* 2021, **23**, 8688-8693.